Journal of Network and Computer Applications 116 (2018) 53–64

Contents lists available at ScienceDirect

Journal of Network and Computer Applications

journal homepage: www.elsevier.com/locate/jnca

Energy-efficient DRX scheduling for D2D communication in 5G networks

Jia-Ming Liang[a,b], Po-Yen Chang[c,f], Jen-Jee Chen[d,*], Chien-Feng Huang[c], Yu-Chee Tseng[c,e]

[a] Department of Computer Science and Information Engineering, Chang Gung University, Taoyuan 33302, Taiwan, ROC
[b] Department of General Medicine, Chang Gung Memorial Hospital, Taoyuan 33378, Taiwan, ROC
[c] Department of Computer Science, National Chiao Tung University, Hsin-Chu 30010, Taiwan, ROC
[d] Department of Electrical Engineering, National University of Tainan, Tainan 70005, Taiwan, ROC
[e] Research Center for Information Technology Innovation, Academia Sinica, Taipei 11574, Taiwan, ROC
[f] Information and Communications Research Laboratories, Industrial Technology Research Institute, Hsinchu 31057, Taiwan, ROC

ARTICLE INFO

Keywords:
Fifth generation (5G)
Device-to-device (D2D) communication
Discontinuous Reception/Discontinuous Transmission (DRX/DTX)
Power saving
Quality of service (QoS)
Resource reuse

ABSTRACT

In recent years, intelligent devices such as smart phones and smart tablets are grown and developed rapidly. High-bandwidth media services such as live streaming, gaming and multi-user video conferencing are more and more popular. This results in spectrum resource depletion of the cellular network. To alleviate the problem, *the 3rd Generation Partnership Project (3GPP)* has proposed a new technology, called *device-to-device (D2D) communications*. However, D2D devices and direct link cellular users all share and access the same spectrum resource, thus degrading the network performance significantly due to the interference. In addition, due to the frequent communication nature of streaming and gaming services, the power consumption of devices is increasing dramatically. To mitigate above problems, this paper investigates how to improve the spectrum efficiency by well scheduling and allocating radio resource to more concurrent D2D and cellular users on the uplink direction and reduce unnecessary power consumption of devices via *Discontinuous Reception (DRX)* scheduling while guaranteeing users' *Quality of Service (QoS)*. We propose an energy-efficient resource and sleep scheduling scheme. This scheme first establishes a conflict graph to maintain the transmission and interference relationship, and then tries to maximize concurrent D2D and mobile users by resource reuse. At the same time, the method also exploits DRX technology to further decrease possible interference and conserve devices' power consumption through optimizing their sleep operation. Simulation results show that our scheme can achieve better performance on system throughput, network capacity, and power saving compared to the existing schemes.

1. Introduction

In recent years, intelligent devices such as smart phones and smart tablets are developed and extensively spread rapidly. High-bandwidth multi-media services such as live streaming (Singh et al., 2016), file sharing (Wang et al., 2015) and video conferencing are getting more and more popular. As a result, the spectrum resource depletion over the cellular network becomes a severe problem (Cao et al., 2016). To support more concurrent devices, *the 3rd Generation Partnership Project (3GPP)* (Astely et al., 2009) has proposed a new technology, called *device-to-device (D2D) communications* (3GPP TS 23.303, 2017; Gandotra and Jha, 2016), to mitigate the spectrum depletion problem. D2D allows direct transmission and reception between two devices without the base station in the middle. This significantly reduces the spectrum access loading of the base station, decreases the network congestion problem (Janis et al., 2009) and increases the spectrum utilization.

However, the D2D communication accesses the same spectrum resource as direct cellular users, thus degrading the transmission efficiency of each device significantly due to the interference (3GPP TS 36.843, 2014). Specifically, when multiple D2D devices access the same uplink resource as the direct uplink mobile user at same time, the transmitters of the ongoing D2D communication pairs will interfere with the reception of the base station; on the contrary, the direct uplink mobile user will also interfere with the receiving of the D2D. Therefore, how to effectively allocate uplink radio resource for D2D communications and cellular users while reducing the mutual interference is a critical issue.

On the other hand, power saving is also an important issue (Solimana and Songb, 2017; Liang et al., 2013). To extend the battery life of devices, the standard has proposed *Discontinuous Reception/Discontinuous Transmission (DRX/DTX)* (3GPP TS 36.331, 2017). When no data needs to be delivered, DRX/DTX allows the device to turn off the wireless access interface and enter into the sleep mode for power

* Corresponding author.
E-mail address: jjchen@mail.nutn.edu.tw (J.-J. Chen).

https://doi.org/10.1016/j.jnca.2018.05.008
Received 13 October 2017; Received in revised form 21 March 2018; Accepted 8 May 2018
Available online 14 May 2018
1084-8045/

saving. However, how to schedule the sleep of devices is an open issue. In this paper, we will show how to schedule and allocate radio resource to improve the network throughput and efficiency via more concurrent D2D and direct cellular user communications on the uplink direction and reduce unnecessary power consumption and interference of devices by exploiting DRX/DTX while ensuring their QoS.

The proposed method includes two phases. In the first phase, we first model a 5G D2D network as a conflict graph $G(V, E)$ according to the interference level between D2D links and between D2D links and the direct links. To guarantee the QoS and maximize the sleep ratio of devices, the sleep cycle of devices are set by referring to the delay constraint. Furthermore, to prevent extra wake-up time of devices because of resource collision, for any two devices, the setting of the sleep cycles follow the exponential increment rule. Then, by jointly consider the conflict graph, sleep cycle of device and the required resource block (RB) sizes, we determine and form spatial reuse groups (SRGs) for D2D and direct link *user equipments (UEs)*, where UEs in the same SRG can share the same RBs. Moreover, UEs in the same SRG will have similar sleep patterns, so later the resource and sleep schedule of SRG can take care of both high resource reuse degree and good power saving. Based on the SRG grouping results of the first phase, the second phase schedules the RB resource and the sleep parameters of each SRG to increase the capacity of the network, guarantee the QoS of services and optimize the power saving of devices. Extensive simulation results show that the proposed scheme can increase radio resource efficiency, raise system throughput and improve power saving effectively.

Major contributions of this paper are threefold. First, this is the first work addressing the joint problem of physical resource allocation and DRX sleep scheduling for D2D communications in 5G networks. Second, we develop a low-complexity and high-efficiency scheduling scheme to elaborate the DRX mechanism with the resource scheduling for D2D and cellular UEs to ensure the QoS requirements while minimizing their energy consumption. We also analyze the time complexity of the proposed scheme to be $O(N^2)$. Third, through the extensive simulation results, it has been validated and shown that the joint problem can be well solved by our proposed scheme and our scheme can save energy significantly as compared to other existing schemes.

The rest of the paper is organized as follows. Section 2 surveys related work. Section 3 introduces the preliminary and formally defines the problem. Section 4 presents the proposed scheme. Numerical results are shown in Section 5. Finally, the conclusion is given in Section 6.

2. Related work

In the literature, several studies have surveyed D2D communication and concluded that D2D can effectively improve the spectrum usage and increase the network throughput. Specifically, the study (Noura and Nordin, 2016) pointed out that interference management techniques can benefit the spectrum reuse and proximity gain. The work (Gandotraa et al., 2017) mentioned that certain architectural enhancements can improve spectral efficiency, energy efficiency and system throughput. The reference (Ahmada et al., 2017) showed that the resource allocation of D2D communications can achieve high data rates, ubiquitous coverage, and low latency. In addition, the research (Lioumpas and Alexiou, 2011) proposed to give different priorities to UEs and suggested to give higher priority to the device with low delay tolerance. However, results show that the performance gain is limited. In reference (Gu et al., 2015), the work proposed to allow a direct link UE and a D2D communication pair to form a resource sharing pair (RSP) and the pair can share the same RBs to increase the throughput of the network. In (Xue and Wen, 2015), the work further proposed to let a D2D communication pair to share resources with multiple direct link UEs. Via satisfying the minimal required signal to interference noise ratio (SINR) of UEs, the system throughput is improved. In reference (Hajiaghayi et al., 2014), this paper proposed to find multiple D2Ds sharing the same RB resources via graph coloring to improve the overall throughput of D2D communications. However, the above studies ignored that multiple direct link UEs and multiple D2D devices can share the same resource concurrently if there is no or only limited interference, especially in the case of large differences in transmission rate. In (Zhang et al., 2015), the paper proposed to decrease the interference between the direct link UE and D2D through fractional power control, thus increasing the network throughput. In references (de Melo et al., 2015a) and (de Melo et al., 2015b), they proposed to improve the system power consumption via their soft dropping power control scheme, which adjusts UE's transmission power to achieve target SINR. In (Asheralieva and Miyanaga, 2016), the work proposed a scheme to meet each user's minimum SINR requirement and guarantee the QoS. The study (Han et al., 2014) proposed the bipartite matching based allocation method, which limits the maximum allowed transmission power by exploiting the minimum SINR requirement, which improved system capacity and power consumption. In (Sultana et al., 2017), a two-stage scheduling approach is proposed to allocate the radio resources by leveraging an adaptive metric with interference, data rate, and transmission power. However, the above studies didn't include DRX mechanism. This makes the network fail to further improve the power saving.

Therefore, based on the above observations, it motivates us to address the resource and sleep scheduling problem in D2D co-existing networks. To the best of our knowledge, this is the first paper to discuss this issue. The objective of the work is to enhance the spectrum utilization, increase the system capacity and reduce the power consumption of UEs while guaranteeing the QoS of services.

3. Preliminary

In this section, we first introduce the D2D communication in 5G networks. Then, we describe the supported traffic features and QoS requirements defined in the standard. Next, we describe the Discontinuous Reception (DRX) mechanism. Finally, we formally define the uplink resource allocation and sleep scheduling problem in 5G D2D networks.

3.1. D2D communication

In 5G networks, there are two types of D2D communications: one is *One-to-One* (Fig. 1(a)(I)) and the other is *One-to-Many* (Fig. 1(a)(II)). The D2D network architecture is shown in Fig. 1(a). *One-to-one* communication is used for *file transfer* and *data sharing applications* (Guo et al., 2016). *One-to-Many* communication is used for *advertisement distribution* and *public safety* (Ali et al., 2016; Kim and Lee, 2015). In the D2D network, D2D devices and the direct link UEs share the uplink radio resource (3GPP TS 36.843, 2014). Therefore, D2D and direct link UEs will interfere with each other. Fig. 1(b) shows an example. In the figure, there are two direct link UEs, UE_1 and UE_2 and three D2D communication groups, $D2D_1$, $D2D_2$ and $D2D_3$. D2D communications may be interfered by direct link UEs if they transmit at the same time and use the same RBs, such as $D2D_1$ and $D2D_3$ are interfered by UE_1 and UE_2 (i.e., $\overrightarrow{I_{u1}}$ and $\overrightarrow{I_{u2}}$), respectively. On the other hand, the uploading direct link UEs are possible to receive the interference at the base station from D2D communications, i.e., $\overrightarrow{I_{d1}}$ and $\overrightarrow{I_{d3}}$. Actually, if the transmission of each device can be properly managed, direct link UEs and D2D communications can transmit without causing interference. For example UE_1 and $D2D_2$ can transmit concurrently without interference, so do UE_2 and $D2D_1$ or UE_2 and $D2D_2$. Therefore, how to schedule the transmission of direct link UEs and D2D devices is an important problem in D2D communication networks. A good schedule can improve the radio resource sharing and avoid interference between devices.

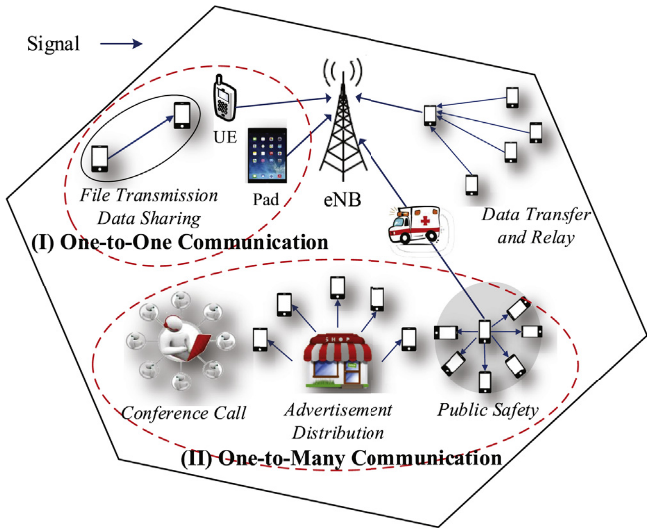

(a) Transmission mode of D2D communication

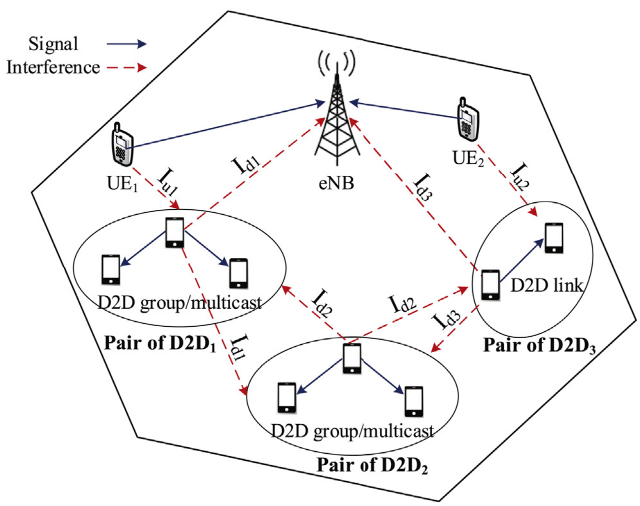

(b) Cellular users and D2D communications coexisting network

Fig. 1. D2D communications and 5G network architecture.

3.2. *Traffic features and QoS requirements in the standard*

The 3GPP standard supports two types of data streams (Alasti et al., 2010): 1) *Guaranteed Bit Rate (GBR)* and 2) *Non-Guaranteed Bit Rate (Non-GBR)* data streams. The GBR stream supports real time streaming service, such as Voice over IP (VoIP), video streaming and gaming. The Non-GBR stream supports non-real time streaming service, such as IP Multimedia Subsystem (IMS) and TCP-based application. According to the current standard, D2D communication is used in real-time proximity communication, conversational voice and file transfer (Lin et al., 2014). Therefore, we primarily focus on the GBR in this paper. The supported *QoS Class Identifier (QCI)* and each of its required delay budget and example services are shown in Table 1. Each GBR stream will have its required QoS needed to be guaranteed.

3.3. *Discontinuous Reception (DRX) mechanism*

The 3GPP standard defines Discontinuous Reception (DRX) and Discontinuous Transmission (DTX) to support sleep mode, which is controlled by the Radio Resource Control (RRC). The central base station (also called the *Evolved Node B, eNB*) can initialize DRX mechanism by sending MAC control signal (3GPP TS 36.321, 2017). Each device

Table 1
Standardized QCI characteristics in the standard (3GPP TS 23.203, 2017).

QCI	Packet Delay Budget	Example Services
1	100 ms	Conversational Voice
2	150 ms	Conversational Video (Live Streaming)
3	50 ms	Real-Time Gaming
4	300 ms	Non-Conversational Video (Buffered Streaming)
5	100 ms	IMS Signaling
6	300 ms	Video (Buffered Streaming), TCP-based (e.g., www, e-mail, chat, ftp, p2p file sharing, progressive video, etc.)
7	100 ms	Voice, Video (Live Streaming), Interactive Gaming
8	300 ms	Video (Buffered Streaming), TCP-based
9	300 ms	Video (Buffered Streaming), TCP-based

† Note that the traffic model of D2D is full buffer and the applications are VoIP and FTP2 with the file size of 10 Kbytes (3GPP TS 36.843, 2014; Luo et al., 2017; 3GPP TS 36.877, 2015).

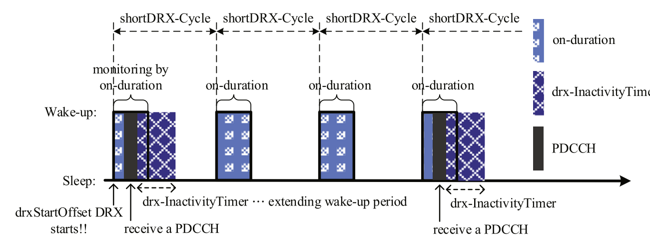

Fig. 2. Overview of the DRX operation.

can operate according to its DRX sleep parameters and all these parameters are configured by eNB. An overview of the DRX operation is shown in Fig. 2. The length of DRX wake-up time and sleep time are in unit of subframes (1 subframe = 1 ms). DRX supports two types of sleep cycles. One is the short cycle; the other is long cycle. Since D2D communications are usually used in real time services, this paper focuses on the DRX short cycle. In DRX, there are four sleep parameters which are used in this work. They are 1) shortDRX-Cycle, 2) on-duration, 3) drxStartOffset and 4) drx-InactivityTimer. ShortDRX-Cycle is the DRX short cycle. On-duration is the least number of wake-up subframes that the UE must keep active at the beginning of a DRX cycle in which the UE monitors the physical downlink control channel (PDCCH). The drxStartOffset is the subframe where the DRX starts. Once the UE receives data packets during on-duration, the UE will start the drx-InactivityTimer. If the UE receives any data packets before the timer expires, the drx-InactivityTimer will be reset; otherwise, the UE will go back to sleep once the timer expires.

Fig. 3 showes the D2D communication setup procedure combined with DRX initialization process. We consider two mobile devices (UE_1 and UE_2), where they will communicate by D2D communication and initiate DRX mechanism. (1) UE_1 and UE_2 will both register to the eNB with the D2D identity (D2D-ID) information by sending RRC connection request. (2) Once UE_1 sends data to UE_2, UE_1 will first send a scheduling request (SR) to the eNB via physical uplink control channel (PUCCH) and then report the buffer status report (BSR) to the eNB by physical uplink shared channel (PUSCH). Except BSR, information such as D2D-ID of UE_2, traffic rate and delay budge will all be included in the message. (3) On the eNB receiving the request, it will assign the D2D transmitter (D2D TX grant) and the D2D receiver (D2D RX grant) resources to UE_1 and UE_2, respectively, via PDCCH. The DRX sleep parameters, including shortDRX-Cycle, on-duration, drx-InactivityTimer and drxStartOffset, are also carried in the message. (4) After step (3), UE_1 and UE_2 can operate according to the received DRX parameters and communicate directly by D2D communication.

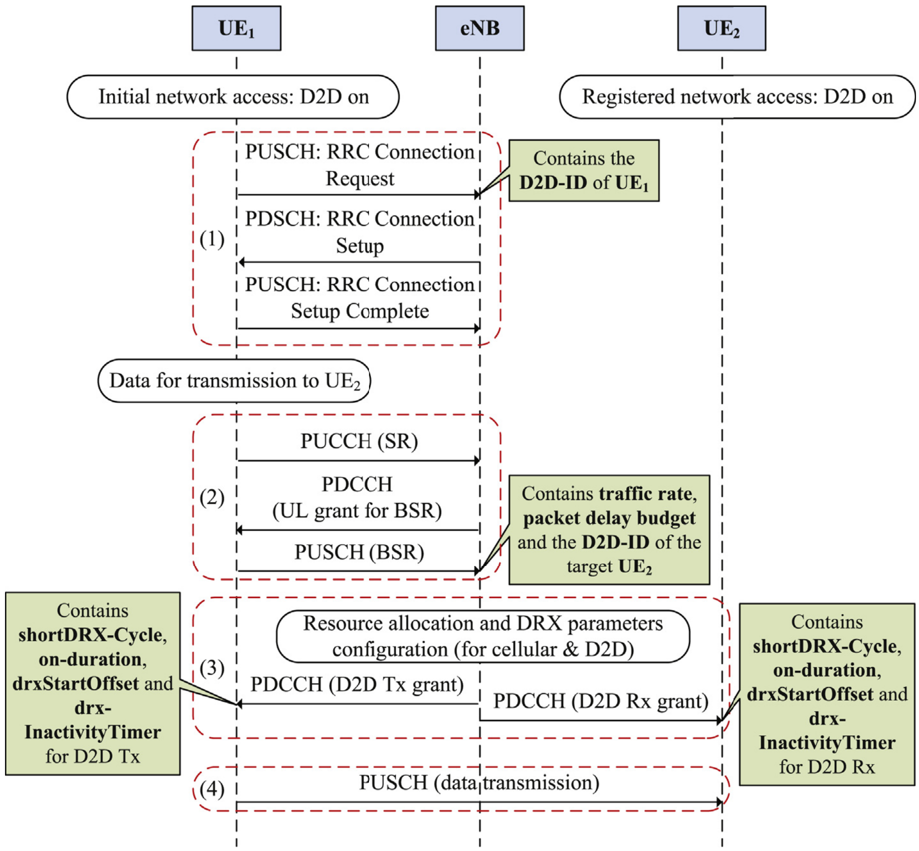

Fig. 3. D2D communication procedures (Tsolkas et al., 2014).

3.4. Problem definition

In this paper, we consider a direct communication (from UE to the eNB) and D2D communication coexisting uplink network. In the network, we assume that there are one eNB and N devices and the network operates under the *FDD* (*frequency division duplex*) mode (3GPP TS 25.214, 2017). In the N devices, n UEs are direct communication UEs and $N - n$ UEs are D2D communication UEs. For each transmitter device Dev_i, we denote its receiver by $Dev_i^R = \{Dev_j\}$, $1 \le |Dev_i^R| \le M$, where Dev_i^R is a receiver set of Dev_i and M is the maximum allowable number of receivers. Each Dev_i has the data rate R_i (in bits/ms) and packet delay budget D_i (in ms). The available bandwidth per uplink subframe is Ω (in resource blocks (RBs)). The channel rate of Dev_i may vary over time (in bits/RB), denoted as $C_i = \min_{j \in Dev_i^R}\{C_{ij}\}$. The channel rate and each of its corresponding modulation and coding scheme (MCS) and required signal to noise ratio (SNR) are shown in Table 2. In this paper, we allow *spatial reuse* which makes a group of D2Ds and a number of direct link UEs share RBs and achieve parallel transmissions. A spatial reuse group is denoted as SRG_x, $x = 1..y$, where y is the total number of spatial reuse groups. The objectives of this paper are to improve the system capacity via enhancing the *spectrum reuse* and reduce the devices' power consumption through sleep scheduling, where the sleep parameters of each UE such as on-duration (T_i^{on}), shortDRX-Cycle (T_i), drxStartOffset (O_i) and drx-InactivityTimer (A_i) have to be determined.

Table 2
Channel Quality Indicator (CQI) supported in the standard (3GPP TS 36.213, 2017).

CQI index	Modulation	Code rate × 1024	Capacity (bits/RB)	SNR Threshold
1	QPSK	78	12.79	< 0
2	QPSK	120	19.69	2.5
3	QPSK	193	31.67	5
4	QPSK	308	50.53	6.5
5	QPSK	449	73.67	9
6	QPSK	602	98.77	11
7	16QAM	378	124.03	17
8	16QAM	490	160.78	17.5
9	16QAM	616	202.13	19
10	64QAM	466	229.36	22
11	64QAM	567	279.07	24
12	64QAM	666	327.79	25
13	64QAM	772	327.79	26
14	64QAM	873	379.97	27
15	64QAM	948	429.68	29

4. The proposed scheme

In this section, we will present our high-efficiency and low-complexity scheme. The flowchart is illustrated in Fig. 4. Specifically, this scheme is composed of two phases. In the first phase, we model the D2D co-existing network as *conflict graph* $G(V, E)$ according to the interference between D2D communications and between D2D and direct link communications. If there is no interference between links, we can group them together and let them transmit at the same time with the same resource to enhance the spectrum efficiency. This phase will also determine the shortDRX-Cycle T_i according to the QoS requirements of each device Dev_i. Then, we use the conflict graph $G(V, E)$, shortDRX-Cycle T_i and data size to jointly determine which devices can form *spatial reuse group (SRG)* to share the same RB. In the second phase, the radio resource assignment of an SRG is based on the maximum number of required radio resource of member devices in the SRG. It iteratively allocates the SRG with the least wasting resource to increase the resource efficiency while guaranteeing the QoS. After resource assignment, we then optimize the DRX parameters for *power saving*. The detail of the proposed scheme is depicted as follows.

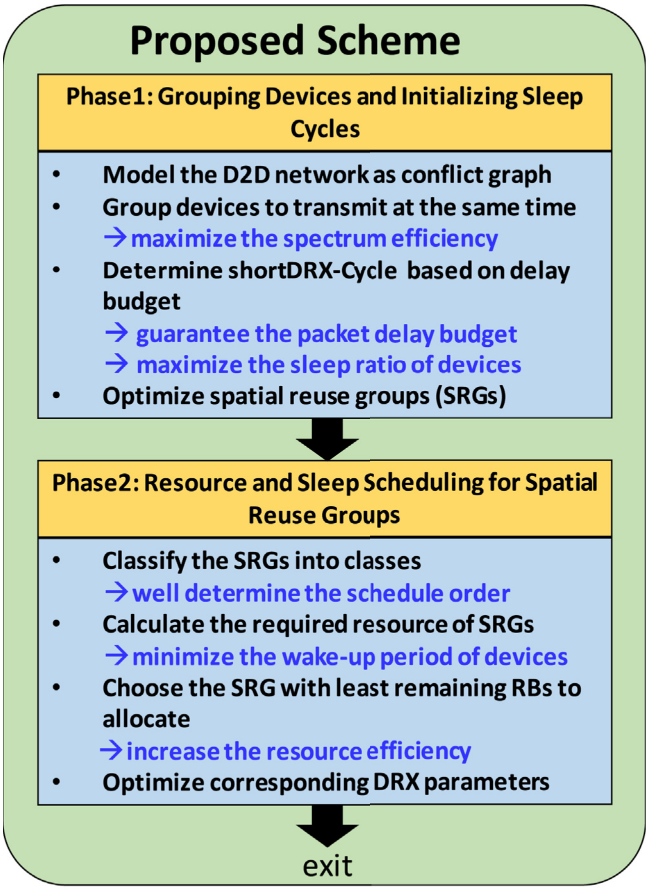

Fig. 4. The flowchart of the proposed scheme.

4.1. Phase1: grouping devices and initializing sleep cycles

The objective of Phase1 is to establish the conflict graph based on the interference relationship between links. After setting up the conflict graph, Phase1 will continue to determine SRGs, where devices in the same SRG can share the same radio resource without causing interference. Then, for each SRG_x, $x = 1 \ldots y$, its sleep cycle will be selected.

Step 1. First, we model the D2D network as a *conflict graph* $G(V, E)$, where $V = \{v_1,\ v_2, \ldots, v_N\}$ and each v_i represents the link of Dev_i and Dev_i^R, and

$$E = \{e_{i,j} | \text{if}(v_i,\ v_j) \text{ causes interference}\}. \tag{1}$$

Therefore, if there exists two vertices v_p and v_q in G which are not connected, means that v_p and v_q can transmit at the same time and share the same resource without any interference.

Step 2. Next, for each device Dev_i, determine the shortDRX-Cycle T_i based on its delay budget D_i and the required amount of RBs. We first sort all Dev_i, $i = 1..N$, in ascending order according to their delay budget D_i. Without loss of generality, let $D_1 \le D_2 \le \cdots \le D_i \le \cdots \le D_N$. T_i is determined by

$$T_i = \begin{cases} D_i, & \text{if } i = 1 \\ \left\lfloor \frac{D_i}{T_{i-1}} \right\rfloor \times T_{i-1}, & \text{if } i = 2..N \end{cases}, \tag{2}$$

where $T_1 = D_1$ can be seen as the DRX basic cycle. Eq. (2) guarantees $T_i \le D_i$ for each Dev_i, $i = 1..N$. In other words, the Dev_i's arrival data is guaranteed to be delivered within T_i. That is, the settings of T_i, $i = 1..N$, guarantee the packet delay budget D_i constraint for each Dev_i. In addition, Eq. (2) makes T_i be an integer multiple of T_j, $j = 1..i-1$. This feature will help to avoid resource competition for devices in the resource scheduling part afterwards. After determining T_i, we then calculate the amount of required RBs for each Dev_i in a T_i cycle, i.e.,

$$RB_i = \left\lceil \frac{R_i \times T_i}{C_i} \right\rceil, \tag{3}$$

where $R_i \times T_i$ (in bits) is the total amount of arrived data size of Dev_i during T_i, C_i (in bits/RB) is the channel rate of Dev_i. Eq. (3) calculates the required number of RBs to guarantee the data rate R_i of Dev_i.

Step 3. Sort all Dev_i, $i = 1 \ldots N$, with positive R_i in ascending order according to their T_i (if there is a tie, sort them according to RB_i in descending order). Without loss of generality, we have the device list L, i.e.,

$$L = (Dev_1,\ \ Dev_2, \cdots, Dev_i),\ \ \forall\ Dev_i \in UE \cup D2D, \tag{4}$$

where UE is the set of cellular transmitters and D2D is the set of D2D transmitters.

Step 4. *Let* SRG_x be the spatial reuse group x, $x = 1..y$, T_x^G and RB_x^G be the sleep cycle length and the maximum required amount of RBs for devices within SRG_x, respectively. Initially, $y = 0$. Then, for each Dev_i in L and $Dev_i \in D2D$, check SRG_x, $x = 1..y$, in sequence. If Dev_i is with the same sleep cycle T_i as $T_{x^*}^G$ and Dev_i is interference-free with SRG_{x^*}, update $SRG_{x^*} = SRG_{x^*} \cup Dev_i$ and $RB_{x^*}^G = \max(RB_{x^*}^G, RB_i)$. On the contrary, if no SRG meets the requirement, create new $SRG_{y+1} = \{Dev_i\}$ and set $y = y + 1$, $T_y^G = T_i$, $RB_y^G = RB_i$. Eq. (5) shows how we find SRG_{x^*} for a device $Dev_i \in D2D$ in L.

Step 5. For each Dev_i in L and $Dev_i \in UE$, check SRG_x, $x = 1..y$, sequentially. If Dev_i is with the same T_i as $T_{x^*}^G$ and Dev_i is interference-free with the D2D links in SRG_{x^*}, do the following. If $RB_{x^*}^G - \sum_{j \in SRG_{x^*}} RB_j \times \Phi_j < RB_i$, where $\Phi_j = 1$ when Dev_j is a cellular transmitter and $\Phi_j = 0$ when Dev_j is a D2D transmitter, then check next SRG; otherwise, set $SRG_{x^*} = SRG_{x^*} \cup Dev_i$. On the contrary, if no SRG can include Dev_i, create new $SRG_{y+1} = \{Dev_i\}$ and update $y = y + 1$, $T_y^G = T_i$, $RB_y^G = RB_i$.

Below, we give an example in Fig. 5 to show the operation of Phase1. We consider the D2D network with one eNB serving 18 devices, which contains 10 direct link UEs and 8 D2D devices, as shown in Fig. 5(a). In Step 1, it establishes the conflict graph based on the interference relationship between direct link UEs and D2D devices, as shown in Fig. 5(b). In Step 2, it determines the shortDRX-Cycle T_i and the amount of required RBs for each device Dev_i, $i = 1..18$. In Step 3, it sorts all Dev_i based on their shortDRX-Cycle T_i and gets the device list L, as shown in Fig. 5(c). In Step 4, it selects the D2D device with the same sleep cycle to SRG_x's and being interference-free with SRG_x and then removes it from L until all devices in L are UEs. Specifically, in the 1st round, it selects Dev_1 (which has shortDRX-Cycle = 100 ms) and creates a new $SRG_1 = \{Dev_1\}$; then, it updates $y = 1$, $T_1^G = T_1$ and $RB_1^G = RB_1$, and removes Dev_1 from L accordingly. In the 2nd round, it selects Dev_2 from L to achieve parallel transmission because Dev_2 has the same shortDRX-Cycle with SRG_1 and also is interference-free with it. Then, it updates $SRG_1 = SRG_1 \cup Dev_2$ accordingly. In the 3rd round, because no other D2D device has the same shortDRX-Cycle with SRG_1 and is interference-free with it, it selects Dev_3 and creates a new $SRG_2 = \{Dev_3\}$. After that, it updates $y = 2$, $T_2^G = T_3$ and $RB_2^G = RB_3$, and then removes Dev_3 from L. The 4th round is done similarly by selecting Dev_4 into SRG_2. For the 5th to 8th rounds, the D2D devices with shortDRX-Cycle = 200 are also selected. Thus, we have $SRG_3 = \{Dev_{13},\ Dev_{14}\}$ and $SRG_4 = \{Dev_5,\ Dev_6\}$, respectively. Therefore, it can find all possible set of D2D links to share the same radio resource. In the 9th round, it selects Dev_8 due to having same shortDRX-Cycle with SRG_1 and SRG_2 (i.e., 100 subframes). However, Dev_8 causes interference to Dev_1 of SRG_1 but is interference-free with all devices of SRG_2. Thus, it adds Dev_8

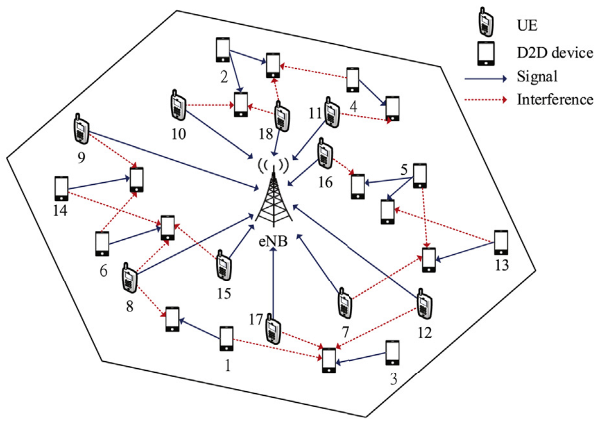

(a) Network topology

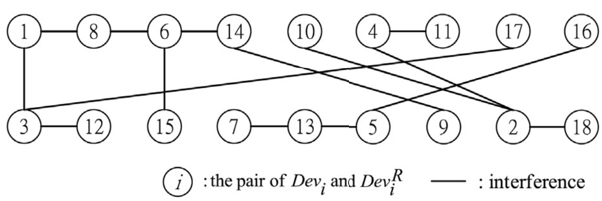

(b) Interference relationship

L = (Dev_1, Dev_3, Dev_2, Dev_8, Dev_{12}, Dev_4, Dev_{10}, Dev_{11}, Dev_{13},

T_i	100	100	100	100	100	100	100	100	200
RB_i	310	250	250	200	150	100	50	50	740

Dev_{14}, Dev_5, Dev_{16}, Dev_{15}, Dev_7, Dev_6, Dev_{17}, Dev_{18}, Dev_9)

200	200	200	200	200	200	200	200	200
500	220	220	210	200	200	160	150	50

(c) Device list L

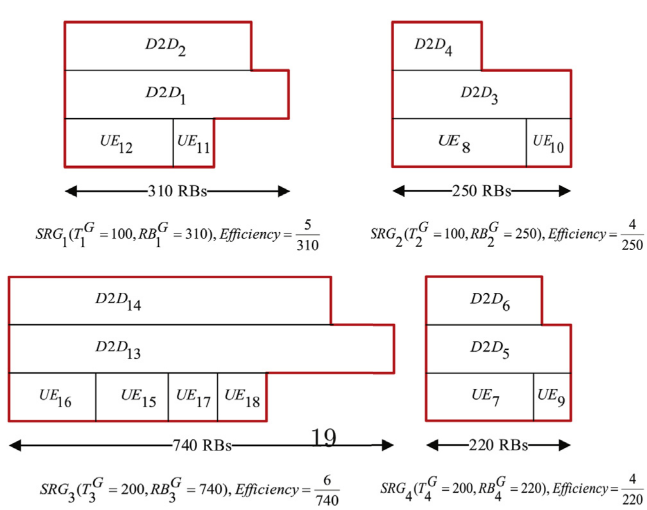

(d) Device grouping

Fig. 5. Operations of Phase1.

to SRG_2 and updates accordingly. In the 10th round, it adds Dev_{12} to SRG_1 because SRG_2 has insufficient resource. In the 11th and 12th rounds, the operations are done similarly by adding Dev_{10} to SRG_2 and Dev_{11} to SRG_1, respectively. These operations repeat in the 13th to 18th rounds, which selects the D2D devices with shortDRX-Cycle = 200. Through the above operations, it can find the minimal number of spatial reuse groups for D2Ds and UEs, as shown in Fig. 5(d), which can improve the spectrum efficiency.

$$SRG_{x^*} = \arg\min_{x=1..y} \{ x \mid T_x^G = T_i, interference\_free(Dev_i, SRG_x), Dev_i \in D2D \text{ in } L \}. \tag{5}$$

4.2. Phase2: resource and sleep scheduling for spatial reuse groups

Based on the SRG grouping results from the first phase, the second phase is to determine each group's optimal schedule, including the subframe index (O_x^G), resource index (I_x^G) and sleep parameters of Dev_i in terms of on-duration (T_i^{on}), shortDRX-Cycle (T_i), and drxStartOffset (O_i). The objective is to increase the total throughput of the system via spatial reuse and conserve the energy of devices via sleep scheduling. The detail of the second phase is depicted as follows.

Step 1. First, we classify the SRGs into S classes ($class_s$, $s = 1..S$). In each $class_s$, every $SRG_x \in class_s$ is with the same T_x^G. For different classes, for example, $class_i$ and $class_j$, the sleep cycle of the members in SRGs in $class_i$ is less than that in $class_j$ if $i < j$. Then, let δ_k be the index of the first subframe with free resource of the kth basic cycle and R_k be the index of the first free RB of the δ_k-th subframe in the kth basic cycle. Initially, $\delta_k = 1$, $R_k = 1$, $k = 1..\left\lceil \frac{T_N}{T_1} \right\rceil$.

Step 2. for each SRG_x, i.e.,

$$ServedNum_x = \sum_{i \in SRG_x} \left| Dev_i^R \right|, \; x = 1..y, \tag{6}$$

where $|Dev_i^R|$ is the total amount of links of Dev_i, if Dev_i's receiver is the eNB, $|Dev_i^R| = |\{eNB\}| = 1$; otherwise, $|Dev_i^R| \geq 1$.

Step 3. From the class with the smallest index, for example $class_{\hat{s}}$, choose the SRG_{x^*} with the maximal average number of receiving devices per RB, i.e.,

$$SRG_{x^*} = \arg\max_{\forall SRG_x \in class_{\hat{s}}} \left\{ \frac{ServedNum_x}{RB_x^G} \middle| SRG_x \in class_{\hat{s}} \right\}. \tag{7}$$

Step 4. To serve SRG_{x^*} with the least subframes, from the 1st DRX basic cycle to the $\left(\frac{T_{x^*}^G}{T_1}\right)^{th}$ DRX basic cycle, choose the one which will leave the minimal number of free RBs at the last allocated subframe after allocate resource to SRG_{x^*}, i.e.,

$$k^* = \arg\min_{k=1..\frac{T_{x^*}^G}{T_1}} \{\Omega - \left(R_k + RB_{x^*}^G - 1\right)\%\Omega \}. \tag{8}$$

Step 5. Then, set $O_{x^*}^G = \delta_{k^*} + (k^* - 1) \times T_1$, $I_{x^*}^G = R_{k^*}$ and update $\delta_{k^*} = \delta_{k^*} + \left\lfloor \frac{R_{k^*} + RB_{x^*}^G - 1}{\Omega} \right\rfloor$, $R_{k^*} = (R_{k^*} + RB_{x^*}^G - 1)\%\Omega + 1$. Remove SRG_{x^*} from $class_{\hat{s}}$ and go back to Step 3. Step 3–5 are repeated until all SRGs are scheduled or resources are exhausted.

We give an example in Fig. 6, which illustrates the optimal schedule for spatial reuse groups. Based on the grouping resulted from Phase1, we have four SRGs: SRG_1, SRG_2, SRG_3 and SRG_4, where the shortDRX-Cycles of those SRGs are $T_1^G = 100$, $T_2^G = 100$, $T_3^G = 200$, $T_4^G = 200$ (subframes) and the number of required RBs are $RB_1^G = 310$, $RB_2^G = 250$, $RB_3^G = 740$, $RB_4^G = 220$ (RBs), respectively. First, in Step 1 of Phase2, it classifies the SRGs into 2 classes (e.g., $class_1$, $class_2$) in ascending order according to T_x^G by $class_1 = \{SRG_1, SRG_2\}$ and $class_2 = \{SRG_3, SRG_4\}$. Next, it calculates the total number of receiving

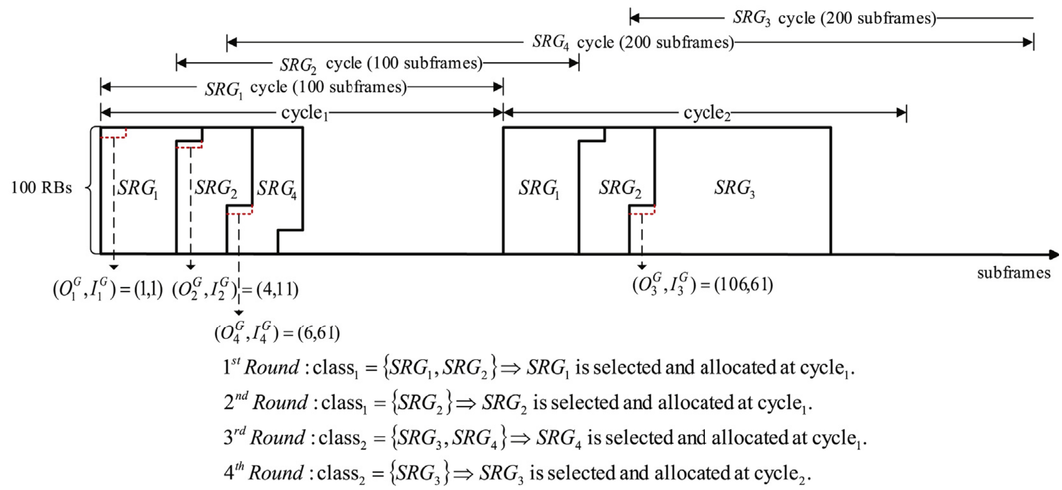

Fig. 6. An example of SRG scheduling.

devices for each SRG_x by Eq. (6) as follows: $ServedNum_1 = 5$, $ServedNum_2 = 4$, $ServedNum_3 = 6$ and $ServedNum_4 = 5$, respectively. Then, it chooses the SRG_x with the maximal average number of receiving devices per RB by Eq. (7) and selects the cycle with the minimal number of free RBs at the last allocated subframe after allocating resource to SRG_x by Eq. (8). Specifically, in the 1st round, it chooses SRG_1 to schedule because it has the maximal number of transmissions per RB (i.e., $\frac{5}{310}$) in $class_1$. Since the scheduling results is the same for basic cycle $k = 1$ and $k = 2$, i.e., $\{100 - (1 + 310 - 1)\%100\} = 90$, it chooses the cycle with the smallest index, i.e., $class_1$, to schedule and sets $O_1^G = 1$ (subframe index) and $I_1^G = 11$ (resource index) for SRG_1. Similarly in the 2nd to 4th rounds, it chooses SRG_2 to schedule in $class_1$, SRG_4 to $class_1$, and SRG_3 to $class_2$ and updates $O_2^G = 4$ and $I_2^G = 11$ for SRG_2, $O_4^G = 6$ and $I_4^G = 61$ for SRG_4, $O_3^G = 106$ and $I_3^G = 61$ for SRG_3, respectively.

Step 6. For each $Dev_i \in D2D$, we determine its sleep parameters and resource allocation. Here we assume $Dev_i \in SRG_x$. Two cases are considered. Case 1: If $I_x^G = 1$, set $O_i = O_x^G$, $I_i = I_x^G$ and $T_i^{on} = \left\lceil \frac{RB_i}{\Omega} \right\rceil$ for $Dev_i \in SRG_x$. Case 2: If $I_x^G \neq 1$, we set Dev_i's sleep parameter and resource allocation following Eq. (9). Above settings guarantee that Dev_i can get the minimal on-duration while satisfying the required resource.

$$\begin{cases} set\ O_i = O_x^G + 1, & I_i = 1 \text{ and } T_i^{on} = \left\lceil \frac{RB_i}{\Omega} \right\rceil \quad \text{if } RB_i \\ & \leq RB_x^G - (\Omega - I_x^G + 1) \\ set\ O_i = O_x^G, & I_i = I_x^G \text{ and } T_i^{on} \\ & = \left\lceil \frac{I_x^G + RB_i - 1}{\Omega} \right\rceil \quad \text{otherwise.} \end{cases} \tag{9}$$

Here, we give an example in Fig. 7 to illustrate the resource allocation order for D2D devices and resource index for SRG_x. Based on the schedule results from Phase2, the SRG_x are considered as two cases. For Case 1, if the resource index is $I_x^G = 1$, such as SRG_1, the resource index is set by $I_i = I_x^G = 1$ for all D2D members in SRG_1, which satisfies $RB_i \leq RB_x^G$ and incurs the minimal wake-up time. Taking $D2D_2$ of SRG_1 as an example, when setting $O_2 = O_1^G = 1$, $I_2 = I_1^G = 1$, it can incur the minimal wake-up time $T_2^{on} = 3$. For Case 2, if the resource index is $I_x^G \neq 1$, such as SRG_2 and SRG_4, it can be further discussed in two cases. If $RB_i \leq RB_x^G - (\Omega - I_x^G + 1)$, the D2D members of SRG_x can incur the minimal wake-up time. We take $D2D_4$ of SRG_2 as an example. Because $RB_4 \leq RB_2^G - (\Omega - I_2^G + 1)$ and can incur the minimal wake-up time, the resource index of $D2D_4$ is set by $I_4 = 1$, $O_4 = 5$ and $T_4^{on} = 1$. Otherwise, if setting the first subframe in SRG_2 for $D2D_4$, i.e., $I_4 = 11$, $O_4 = 4$ and $T_4^{on} = 2$, this cannot incur the minimal wake-up time. Therefore, through the above Cases 1 and 2, it can make sure that the D2D members of SRG_x have the minimal wake-up time.

Step 7. For each SRG_x, determine cellular UEs' sleep parameters and resource allocation as follows. First, we find the target device Dev_{i^*} according to the following Eq. (10). If such Dev_{i^*} exists, set $O_{i^*} = O_x^G$, $I_{i^*} = I_x^G$ and $T_i^{on} = \left\lceil \frac{RB_{i^*}}{\Omega} \right\rceil$. Then, update $O_x^G = O_x^G + \left\lfloor \frac{I_x^G + RB_{i^*} - 1}{\Omega} \right\rfloor$, $I_x^G = (I_x^G + RB_{i^*} - 1)\%\Omega + 1$ and mark Dev_{i^*} as allocated. On the contrary, if such Dev_{i^*} does not exist, we find the target device Dev_{i^*} by following alternative way.

$$i^* = \arg\min_i \left\{ (I_x^G + RB_i - 1)\%\Omega \;\middle|\; \text{if} \left\lceil \frac{RB_i}{\Omega} \right\rceil = \left\lceil \frac{I_x^G + RB_i - 1}{\Omega} \right\rceil, Dev_i \in UE \text{ in } SRG_x \right\}. \tag{10}$$

$$i^* = \arg\min_i \{(I_x^G + RB_i - 1)\%\Omega \mid Dev_i \in UE \text{ in } SRG_x\}. \tag{11}$$

Then, set $O_{i^*} = O_x^G$, $I_{i^*} = I_x^G$, $T_{i^*}^{on} = \left\lceil \frac{I_x^G + RB_{i^*} - 1}{\Omega} \right\rceil$ and update $O_x^G = O_x^G + \left\lfloor \frac{I_x^G + RB_{i^*} - 1}{\Omega} \right\rfloor$, $I_x^G = (I_x^G + RB_{i^*} - 1)\%\Omega + 1$. Dev_{i^*} is marked as allocated. The above operation will be repeated until all cellular UEs in SRG_x are marked.

Step 8. For each device, set drx-InactivityTimer to be 1 (Liang et al., 2016), i.e., $A_i = 1$, $i = 1..N$. After completing above steps, we can make devices obtain shorter on-duration (T_i^{on}) and set their drxStartOffset (O_i), resource index (I_i), and drx-InactivityTimer (A_i) ready to achieve better energy efficiency.

Below, we give an example in Fig. 8 to illustrate the resource allocation order of UE members and resource index for SRG_x. Consider the scheduling result of SRG_3 from previous example, the 1st round selects UE_{15} by Eq. (10) because it can incur the minimal wake-up time and have the minimal number of free RBs at the last allocated subframe. Then, it sets the resource index for UE_{15} by $I_{15} = I_3^G = 61$, $O_{15} = O_3^G = 106$, $T_{15}^{on} = 3$, and updates $O_3^G = 108$, $I_3^G = 71$ accordingly. Similarly, the 2nd round selects UE_{16} and sets $I_{16} = I_3^G = 71$, $O_{16} = O_3^G = 108$, $T_{16}^{on} = 3$, and then updating $O_3^G = 110$, $I_3^G = 91$. In the 3rd round, because there is no UE which can incur the minimal wake-up time, it chooses UE_{18} according to Eq. (11), which has the minimal number of free RBs at the last allocated subframe that may make more UEs to have the minimal wake-up time. Then, it sets the resource index

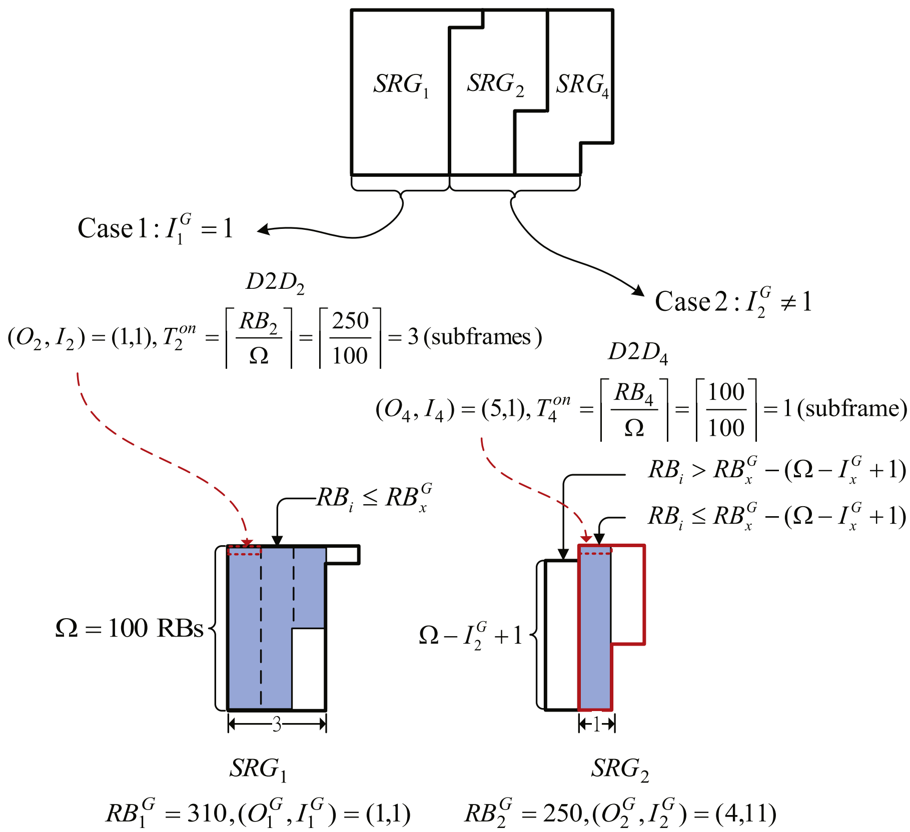

Fig. 7. An example of determining the DRX startOffset of D2D devices in SRG.

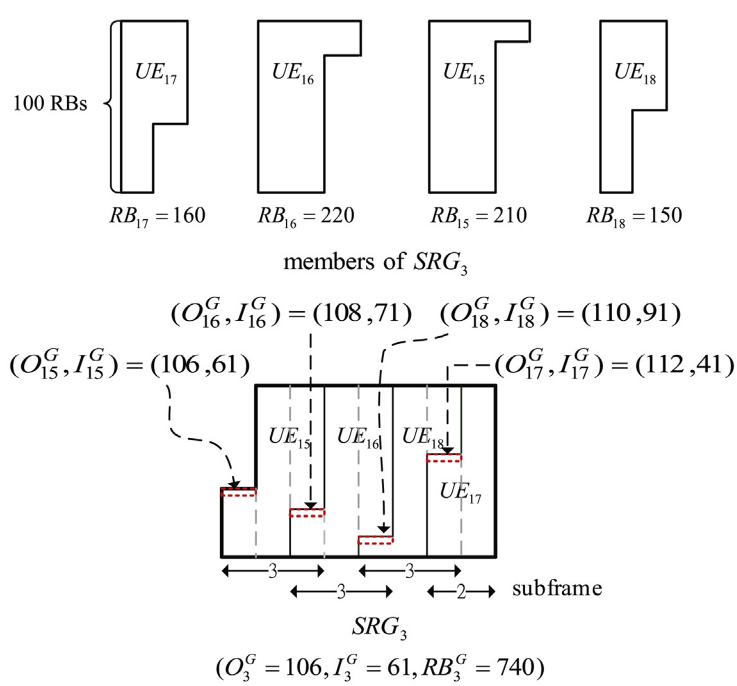

1^{st} *Round* : UE_{15} is selected and set $O_{15} = 106, I_{15} = 61, T_{15}^{on} = 3$, updates $O_3^G = 108, I_3^G = 71$.

2^{nd} *Round* : UE_{16} is selected and set $O_{16} = 108, I_{16} = 71, T_{16}^{on} = 3$, updates $O_3^G = 110, I_3^G = 91$.

3^{rd} *Round* : UE_{18} is selected and set $O_{18} = 110, I_{18} = 91, T_{18}^{on} = 3$, updates $O_3^G = 112, I_3^G = 41$.

4^{th} *Round* : UE_{17} is selected and set $O_{17} = 112, I_{17} = 41, T_{17}^{on} = 2$, updates $O_3^G = 114, I_3^G = 1$.

Fig. 8. An example of determining the DRX parameters of UEs in SRGs.

for UE_{18} by $I_{18} = I_3^G = 91$, $O_{18} = O_3^G = 110$, $T_{18}^{on} = 3$, and updates $O_3^G = 112$, $I_3^G = 41$ accordingly. Finally, in the 4th round, UE_{17} is selected similarly.

4.3. Analysis of time complexity

In the proposed scheme, it works in two phases. In the first phase, the step 1 costs $O(N^2)$ to construct a conflict graph because there are at most N vertexes (i.e., links of devices) and each may establish a link (i.e., causing interference) to other $N-1$ vertexes. The step 2 first costs $O(N)$ to determine the shortDRX-Cycle for N devices and costs $O(N \log N)$ to sort devices according to their delay budgets. Then, it costs $O(N)$ to calculate the amount of required RBs for N devices. Thus, the step 2 totally costs $O(N) + O(N \log N) + O(N) = O(N \log N)$. The step 3 costs $O(N \log N)$ to sort N devices in ascending order according to their cycle lengths. The step 4 costs $O(N^2)$ for at most N D2D devices and each needs to check N spatial reuse groups if it is interference free with them; if not, it then costs extra $O(1)$ to create a new SRG. The step 5 costs $O(N^2)$ for at most N UEs and each checks at most N SRGs if the total length is over the group size; if yes, it then costs additional $O(1)$ to create a new SRG. Therefore, the phase 1 totally costs $O(N^2) + O(N \log N) + O(N \log N) + O(N^2 + 1) + O(N^2 + 1) = O(N^2)$.

In the second phase, the step 1 first costs $O(N \log N)$ to classify at most N SRGs and sort them according to their cycle lengths. Then, it costs $O(T_N/T_1)$ to initialize the index of free RBs for T_N/T_1 cycles. Thus, the step 1 totally costs $O(N \log N) + O(T_N/T_1) = O(N \log N)$. The step 2 costs $O(N^2)$ to sum up the number of served devices for all SRGs, where there are at most N SRGs and each SRG contains at most N devices. The step 3 costs $O(N)$ to find the SRG with the maximal average number of receiving devices per RB. The step 4 costs $O(T_N/T_1)$ to choose the cycle with the least subframe among T_N/T_1 cycles. The step 5 costs $O(1)$ to set the index of subframes and RBs for the SRG chosen from step 2. Then, steps 3 ~ 5 are repeated at most $O(N)$ times until all SRGs are scheduled. Thus, steps 3 ~ 5 totally cost $O(N) \times (O(N) + O(T_N/T_1) + O(1)) = O(N^2)$. The step 6 costs $O(N)$ to determine the allocation index of subframes and RBs for at most N D2D devices. The step 7 costs $O(N^2)$ to determine the allocation index of subframes and RBs for at most N UEs, where each UE is with the minimal number of remaining RBs after allocating in an SRG. The step 8 costs $O(N)$ to determine the InactivityTimer of N devices. Therefore, the phase 2 totally costs $O(N \log N) + O(N^2) + O(N^2) + O(N) + O(N^2) + O(N) = O(N^2)$.

In brief, the time complexity of the proposed scheme incurred by the two phases is $O(N^2) + O(N^2) = O(N^2)$.

5. Numerical results

We develop a simulator in C + + language to verify the effectiveness of the proposed scheme.[1] The system parameters in our simulation are listed in Table 3 (3GPP TS 25.214, 2017). The network contains one eNB and 100 ~ 2000 devices, where these devices contain direct link UEs and D2D devices, and the ratio is 2:1. The channel rates of the UE and the D2D devices are determined by the distance between the UE and the eNB and between the D2D transmitter and receiver, respectively. Note that the UEs are deployed uniformly and apply random walk mobility model with the speed of 1.4 m/s (Deng et al., 2016).

Since the standard does not provide a specific method for D2D scheduling, we compare our scheme against the most related schemes from the literature, including ***Proportional Fairness Scheme (PFS)*** (Gu et al., 2015), the ***Multi-user Resource Multiplexing Scheme (MRMS)*** (Xue and Wen, 2015), the ***Opportunistic Scheme (OPP)*** (Hajiaghayi et al., 2014), and the ***Adaptive Resource Allocation Scheme (ADR)*** (Sultana et al., 2017). **PFS** allocates consecutive RBs to resource sharing pairs to provide better transmission quality. **MRMS** allows one D2D and multiple UEs to share the wireless resource. **OPP** clusters D2D communications into groups and makes multiple D2D communications to share wireless resource. Moreover, OPP prioritizes the scheduling of clustered groups with higher throughput to improve performance. Finally, **ADR** allocates the resource for D2D and UEs by an adaptive metric with interference, data rate, and transmission power under the physical constraints.

Table 3
System parameters (3GPP TS 25.214, 2017).

Simulation Parameter	Value
Channel bandwidth	20 MHz
Number of RBs per subframe	100
Cell radius	500 m
Number of devices	100 ~ 2000
Transmission power (fixed)	23 dBm
Distance between D2D	20 m
UE path loss model	128 + 37.6·log(r), r in km
D2D path loss model	148 + 40·log(r), r in km
Delay budget	100, 300 ms
UE request size	13, 26, 34 kbps
D2D request size	64, 128, 169 kbps

5.1. System throughput

We investigate the effect of the number of devices on the system throughput. In Fig. 9, we can see that when the number of devices increases, the system throughput increases. PFS has the worst performance because it limits the resource sharing by single UE and D2D device. Since MRMS allows the wireless resource sharing between one D2D and multiple UEs, it performs better than PFS. OPP uses clustering to share the wireless resource for more D2Ds, therefore OPP has a higher throughput than MRMS. The performance of ADR scheme is better than them because it can allocate resource adaptively based on the physical status. Note that our scheme outperforms all other schemes because our scheme can group more devices based on the conflict graph and efficiently schedule resource based on the remaining space when scheduling SRGs.

5.2. Number of served devices

We then investigate the effect of the number of requesting devices on the average number of served devices. In Fig. 10, we can see that the average number of served devices increases when the number of requesting devices increases, except for PFS. This is because PFS shares the wireless resource only between single D2D and UE. MRMS performs better than PFS because MRMS shares more resource between D2D and multiple UEs. Since OPP clusters D2D communications to improve transmission efficiency, it can have higher performance than MRMS. ADR scheme outperforms all the above schemes because its adaptive mechanism can find more suitable members of spatial reuse groups according to the devices' physical status. Note that our scheme can achieve the highest performance because our scheme can optimize the spatial reuse groups in phase 1 and fully reuse spectrum by packing SRGs with the least remaining space in phase 2.

5.3. Successful scheduling ratio

Next, we investigate the effect of the number of devices on the successful scheduling ratio. In Fig. 11, we can see that when the number of devices increases, the successful scheduling ratio decreases due to network saturation. Similarly, PFS has the worst successful scheduling ratio because PFS shares least resource and thus more UEs cannot be served successfully. MRMS and OPP perform better than PFS because

[1] Currently, the well-known simulator, such as *ns-3* (NS-3 Consortium, 2018), only supports the procedure of device discovery for D2D communications. The physical module of the D2D communication has not been supported completely.

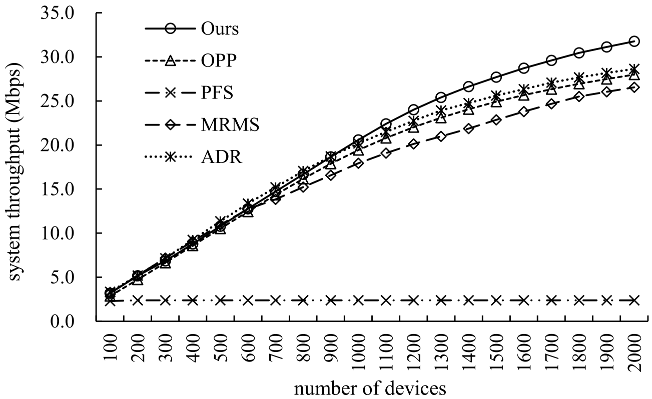

Fig. 9. Impact of number of devices on system throughput.

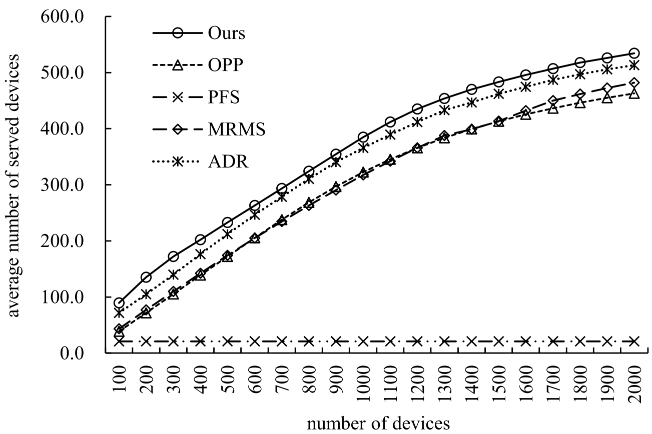

Fig. 10. Impact of number of devices on average number of served devices.

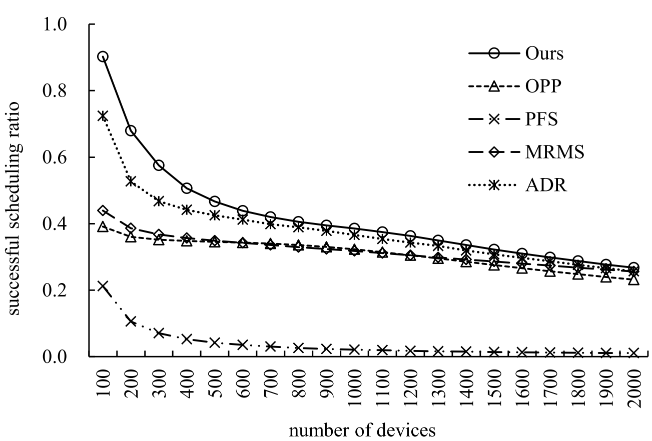

Fig. 11. Impact of number of devices on successful scheduling ratio.

they can share more resource between UEs and D2D devices. The performance of ADR scheme is better than the above schemes because it can well share resource according to the adaptive metric. Note that our scheme has higher successful scheduling ratio especially when the number of devices ranges from 100 to 1100, where the improvement by our scheme is up to 25% as compared to other schemes. This is because our scheme can determine the best cycle length without violating devices' delay budget. Thus, more devices' QoS can be satisfied.

5.4. Average transmission bit per RB

In Fig. 12, we investigate the effect of the number of devices on the average transmission bits per RB. As can be seen, the average bits per

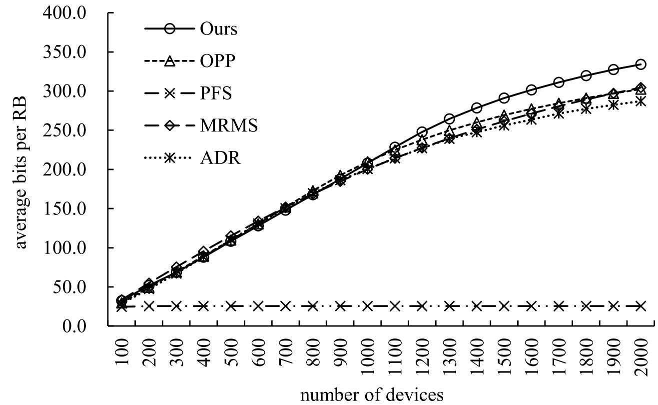

Fig. 12. Impact of number of devices on average transmission bits per RB.

RB of most schemes increases when the number of devices increases. The performance of PFS is the lowest due to singular resource sharing. MRMS, OPP, and ADR have lower average bits per RB because they may not fully leverage spectrum reuse for the D2D and UE links, thus limiting the performance. It is worth noting that our scheme outperforms all other schemes because our scheme can well share resource by considering the total amount of links, therefore achieving higher performance.

5.5. Sleep ratio

Next, we investigate the effect of the number of devices on the average sleep ratio. In Fig. 13, we can see that when the number of devices increases, the average sleep ratio decreases. PFS, MRMS, OPP, and ADR have the worse average sleep ratio because they do not employ DRX and their data reception do not contain periodic features, so devices need to keep waking up for possible data delivery. For our proposed scheme, when the number of devices increases, the average sleep ratio slightly decreases. The reason is that our scheme has to ensure the quality of service for the devices by reserving the basic requirement RBs for each device. Therefore, when the number of devices increases, amount of available resource decreases, thus reducing the sleep time of devices.

5.6. Power consumption

Here, we investigate the effect of the number of devices on the average power consumption. The calculation of the power consumption for direct link UEs and D2Ds are based on Fig. 15. As shown in Fig. 14, we can see that when the number of devices increases, the average power consumption per device increases. Similarly, PFS, MRMS, OPP,

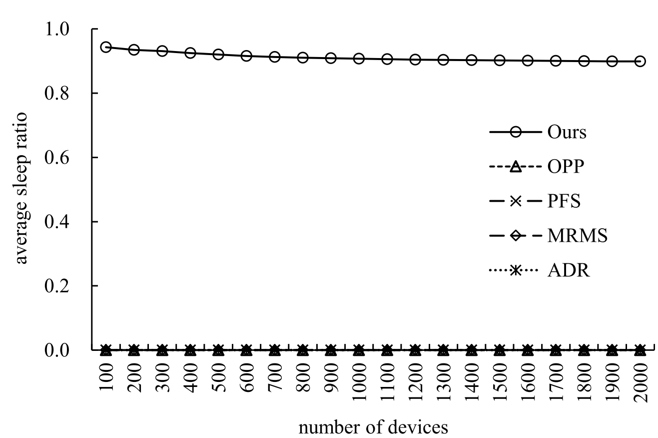

Fig. 13. Impact of number of devices on average sleep ratio.

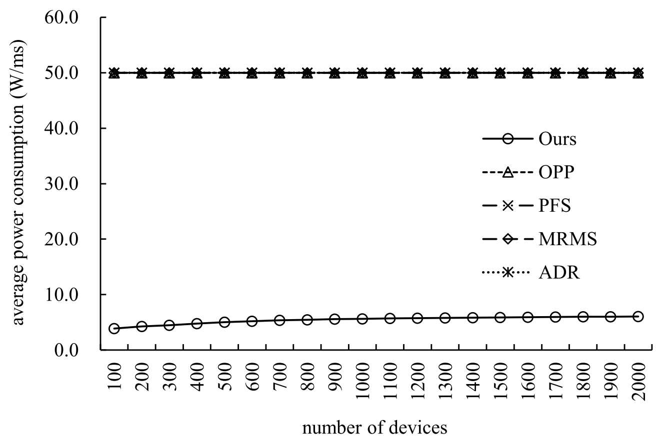

Fig. 14. Impact of number of devices on average power consumption.

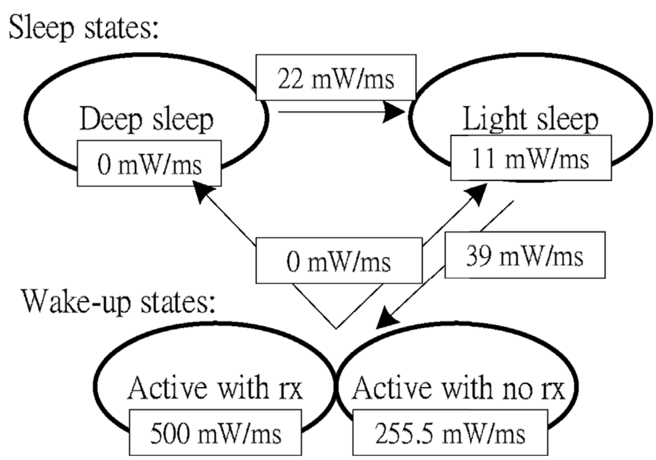

Fig. 15. The power consumption model. (3GPP TSG RAN, 2007).

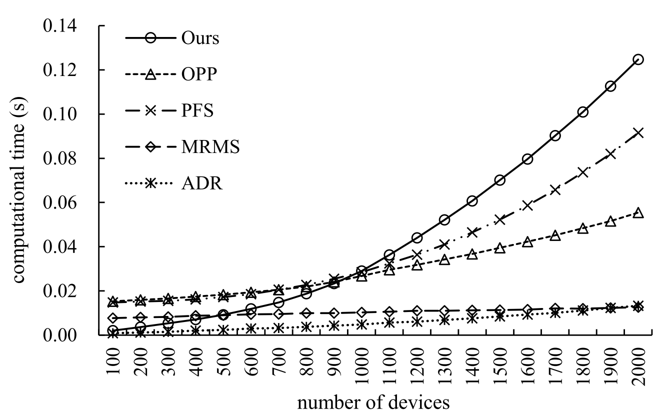

Fig. 16. Impact of number of devices on computational time.

and ADR incur the most power consumption because these devices need to keep waking up to wait for possible data delivery. Our scheme has least average power consumption because we apply DRX mechanism and optimize the sleep parameters appropriately. Thus, data delivery and resource scheduling are well determined and follow the regular wake-up and sleep patterns. This effectively reduces the wake-up time and power consumption of devices.

5.7. Computational time

Finally, we investigate the effect of the number of devices on the computational time. The time is measured by the platform of Dell 990 with Intel i7-2600 3.4 GHz and DDR3-1600 16 GB. As shown in Fig. 16, the computational time of most schemes increases when the number of devices increases. Comparing with our scheme, PFS, MRMS, OPP, and ADR have lower computational time because they neglect to guarantee the QoS requirement of devices and may not fully utilize the spectrum of the D2D and UE links. Our scheme has higher computational time because it needs more time to parallel transmissions and calculate the best sleep parameters to guarantee devices' QoS. Fortunately, the total computational time of our scheme is still less than 1 s even when the number of devices increase up to 2000, which is much less than the scheduling period (i.e., few seconds).

6. Conclusion

In this paper, we propose an energy-efficient DRX scheduling scheme for D2D communication in 5G networks. We address the physical resource block allocation and DRX sleep scheduling problem where the QoS requirements of D2D communications and direct link UEs must be ensured. An efficient two-phase scheme is proposed to tackle the problem. This scheme first establishes a conflict graph to maintain the interference relationship of the network and then tries to maximize the resource reuse between D2D and direct link UEs. In addition, our scheme also exploits DRX technology to conserve devices' energy while decrease the interference of the network. Simulation results show that our scheme can enhance the system throughput and save devices' power consumption while guarantee their QoS requirements.

Acknowledgments

This research is co-sponsored by MOST 106-2221-E-024-004-, 102-2218-E-182-008-MY3, 105-2221-E-182-051, 106-2221-E-182-015-MY3, 105-2745-8-182-001, 106-2221-E-024-004, 105-2221-E-009-100-MY3, 105-2218-E-009-029, 105-2923-E-009-001-MY2, 104-2221-E-009-113-MY3, MoE ATU Plan, Delta Electronics, ITRI, Institute for Information Industry, Academia Sinica AS-105-TP-A07, and Chang Gung Memorial Hospital, Taoyuan.

References

3GPP TS 23.203, September 2017. Policy and Charging Control Architecture, v15.0.0 (Release 15).
3GPP TS 23.303, June 2017. Proximity-based Services (ProSe); Stage 2, v15.0.0 (Release 15).
3GPP TS 25.214, September 2017. Physical Layer Procedures (FDD), v15.0.0 (Release 15).
3GPP TS 36.213, September 2017. E-UTRA; Physical Layer Procedures, v14.4.0 (Release 14).
3GPP TS 36.321, September 2017. E-UTRA; Medium Access Control (MAC) Protocol Specification, v14.4.0 (Release 14).
3GPP TS 36.331, September 2017. E-UTRA; Radio Resource Control (RRC) Protocol Specification, v14.4.0 (Release 14).
3GPP TS 36.843, March 2014. Study on LTE Device to Device Proximity Services; Radio Aspects, v12.0.0 (Release 12).
3GPP TS 36.877, March 2015. LTE Device to Device Proximity Services; User Equipment (UE) Radio Transmission and Reception, v12.0.0 (Release 12).
3GPP TSG RAN, March 2007. WG2 LTE Contribution, R2-071285, DRX Parameters in LTE.
Ahmada, M., Azamb, M., Naeema, M., Iqbala, M., Anpalaganc, A., Haneefb, M., 2017. Resource management in D2D communication: an optimization perspective. J. Netw. Comput. Appl. 93, 51–75.
Alasti, M., Neekzad, B., Hui, J., Vannithamby, R., 2010. Quality of service in WiMAX and LTE networks. IEEE Commun. Mag. 48 (5), 104–111.
Ali, K., Nguyen, H.X., Shah, P., Vien, Q.T., Bhuvanasundaram, N., 2016. Architecture for public safety network using D2D communication. In: IEEE Wireless Communications and Networking Conference (WCNC), pp. 1–6.
Asheralieva, A., Miyanaga, Y., 2016. QoS-oriented mode, spectrum, and power allocation for D2D communication underlaying LTE-a network. IEEE Trans. Veh. Technol. 65 (12), 9787–9800.
Astely, D., Dahlman, E., Furuskär, A., Jading, Y., Lindström, M., Parkvall, S., 2009. LTE: the evolution of mobile Broadband. IEEE Commun. Mag. 47 (4), 44–51.
Cao, Y., Long, C., Jiang, T., Mao, S., 2016. Share communication and computation resources on mobile devices: a social awareness perspective. IEEE Wirel. Commun. 23

(4), 52–59.
de Melo, Y.V.L., Batista, R.L., e Silva, C.F.M., Maciel, T.F., da Silva, J.M.B., Cavalcanti, F.R.P., 2015a. Uplink power control with variable target SINR for D2D communications underlying cellular networks. In: IEEE Vehicular Technology Conference (VTC), pp. 1–5.
de Melo, Y.V.L., Batista, R.L., e. Silva, C.F.M., Maciel, T.F., da Silva, J.M.B., Cavalcanti, F.R.P., 2015b. Power control schemes for energy efficiency of cellular and device-and-device communications. In: IEEE Wireless Communications and Networking Conference (WCNC), pp. 1690–1694.
Deng, T., Wang, X., Fan, P., Li, K., 2016. Modeling and performance analysis of tracking area list-based location management scheme in LTE networks. IEEE Trans. Veh. Technol. 65 (8), 6417–6431.
Gandotra, P., Jha, R.K., 2016. Device-to-Device communication in cellular networks: a survey. J. Netw. Comput. Appl. 71 (1), 99–117.
Gandotraa, P., Jhaa, R.K., Jain, S., 2017. A survey on device-to-device (D2D) communication: architecture and security issues. J. Netw. Comput. Appl. 78, 9–29.
Gu, J., Yoon, H., Lee, J., Jae Bae, S., Young Chung, M., 2015. A resource allocation scheme for device-to-device communications using LTE-a uplink resources. ELSEVIER Pervasiv. Mobile Comput. 18 (3), 104–117.
Guo, Y., Duan, L., Zhang, R., 2016. Cooperative local caching and file sharing under heterogeneous file preferences. In: IEEE International Conference on Communications (ICC), pp. 1–6.
Hajiaghayi, M., Wijting, C., Ribeiro, C., Hajiaghayi, M.T., 2014. Efficient and practical resource block allocation for LTE-based D2D network via graph coloring. Wireless Network 20 (4), 611–624.
Han, J., Cui, Q., Yang, C., Valkama, M., Tao, X., 2014. Optimized power allocation and spectrum sharing in device to device underlaying cellular systems. In: IEEE Wireless Communications and Networking Conference (WCNC), pp. 1332–1337.
Janis, P., Yu, C.-H., Doppler, K., Ribeiro, C., Wijting, C., Hugl, K., Tirkkonen, O., Koivunen, V., 2009. Device-to-Device communication underlaying cellular communications systems. Int. J. Commun. Netw. Syst. Sci. 2 (3), 169–178.
Kim, J., Lee, H., 2015. Geographical proximity based target-group formation algorithm for D2D advertisement dissemination. In: IEEE International Conference on Pervasive Computing and Communication Workshops (PerCom), pp. 272–275.
Liang, J.-M., Chen, J.-J., Cheng, H.-H., Tseng, Y.-C., 2013. An energy-efficient sleep scheduling with QoS consideration in 3GPP LTE-advanced networks for Internet of Things. IEEE J. Emerg. Select. Top. Circ. Syst. 3 (1), 13–22.
Liang, J.-M., Chen, J.-J., Hsieh, P.-C., Tseng, Y.-C., 2016. Two-phase multicast DRX scheduling for 3GPP LTE-advanced networks. IEEE Trans. Mobile Comput. 15 (7), 1839–1849.
Lin, X., Andrews, J.G., Ghosh, A., Ratasuk, R., 2014. An overview of 3GPP device-to-device proximity services. IEEE Commun. Mag. 52 (4), 40–48.
Lioumpas, A.S., Alexiou, A., 2011. Uplink scheduling for machine-to-machine communications in LTE-based cellular systems. In: IEEE Global Communications Conference (GLOBECOM), pp. 353–357.
Luo, R.S.Y., Hong, P., Xue, K., 2017. Resource allocation for energy harvesting-powered D2D communication underlaying cellular networks. IEEE Trans. Veh. Technol. 66 (11), 10486–10498.
Noura, M., Nordin, R., 2016. A survey on interference management for device-to-device (D2D) communication and its challenges in 5G networks. J. Netw. Comput. Appl. 71, 130–150.
NS-3 Consortium, 2018. ns-3 Network Simulator. https://www.nsnam.org/.
Singh, S., Saxena, N., Roy, A., De, P., 2016. Proximity-based video delivery architecture for LTE networks. Electron. Lett. 52 (11), 984–986.
Solimana, S.S., Songb, B., 2017. Fifth generation (5G) cellular and the network for tomorrow: cognitive and cooperative approach for energy savings. J. Netw. Comput. Appl. 85 (1), 84–93.
Sultana, A., Zhao, L., Member, S., Fernando, X., 2017. Efficient resource allocation in device-to-device communication using cognitive radio technology. IEEE Trans. Veh. Technol. 66 (11), 10024–10034.
Tsolkas, D., Liotou, E., Passas, N., Merakos, L., 2014. Lte-a access, core, and protocol architecture for D2D communication. Smart Dev. Smart Device Commun. 23–40.
Wang, L., Gao, L., Zhang, A., Chen, M., 2015. Social-aware file-sharing mechanism for device-to-device communications. In: International Conference on Wireless Communications Signal Processing (WCSP), pp. 1–5.
Xue, J., Wen, B., 2015. Resource allocation for device-to-device communication underlaying LTE networks. IEEE J. Comput. Inf. Syst. 11, 75–86.
Zhang, Z., Hu, R.Q., Qian, Y., Papathanassiou, A., 2015. D2D communication underlay in uplink cellular networks with fractional power control and fractional frequency reuse. In: IEEE Global Communications Conference (GLOBECOM), pp. 1–7.